Brain Pathology ISSN 1015-6305

RESEARCH ARTICLE

Tau-Tubulin Kinase 1 Expression, Phosphorylation and Co-Localization with Phospho-Ser422 Tau in the Alzheimer's Disease Brain

Harald Lund[1,2]; Richard F. Cowburn[1]; Elin Gustafsson[1]; Kia Strömberg[1,3]; Anne Svensson[1]; Leif Dahllund[1]; David Malinowsky[1]; Dan Sunnemark[1,2]

[1] Neuroscience Department, AstraZeneca R&D, Södertälje, Sweden.
[2] Department of Clinical Neuroscience, Center for Molecular Medicine L8:04, Karolinska Institute, Stockholm, Sweden.
[3] Science for Life Laboratory, Division of Translational Medicine and Chemical Biology, Department of Medical Biochemistry and Biophysics, Karolinska Institute, Stockholm, Sweden.

Keywords
Alzheimer's disease, neurofibrillary tangles, tau phosphorylation, tau-tubulin kinase 1.

Corresponding author:
Harald Lund, MSc, Department of Clinical Neuroscience, Center for Molecular Medicine L8:04, Karolinska Institute, 171 76 Stockholm, Sweden (E-mail: *harald.lund@ki.se*)

Received 6 July 2012
Accepted 17 October 2012
Published Online Article Accepted 23 October 2012

doi:10.1111/bpa.12001

Abstract

Recent reports have implicated tau-tubulin kinase 1 (TTBK1) in the pathological phosphorylation of tau that occurs in Alzheimer's disease (AD).

The present study was undertaken to provide an extensive characterization of TTBK1 mRNA and protein expression in human brain from AD cases and non-demented controls so as to better understand the disease relevance of this novel kinase. *In situ* hybridization and immunohistochemistry revealed abundant expression of TTBK1 in the somatodendritic compartment of cortical and hippocampal neurons of both AD cases and controls. TTBK1 immunoreactivity appeared to vary with the level of phospho-tau staining, and was strong in the somatodendritic compartment of apparently healthy hippocampal neurons as well as in pre-tangle neurons where it co-localized with diffuse phospho-Ser422 tau staining. Ser422 was confirmed as a TTBK1 substrate *in vitro*, and an antibody towards the site, in addition to labeling AT8-positive neurofibrillary tangles (NFTs), neuritic plaques and neuropil threads, also labeled a small population of neurons that were unlabeled with AT8.

These data suggest a role for TTBK1 in pre-tangle formation prior to the formation of fibrillar tau and strengthen the idea that tau is phosphorylated at Ser422 at an early/intermediate stage in NFT formation.

INTRODUCTION

Hyperphosphorylated tau protein has long been known as the major component of paired helical filaments (PHFs) that constitute the characteristic Alzheimer's disease (AD) pathologies of neuritic changes and neurofibrillary tangles (NFTs) (6). Tau phosphorylation occurs at over 50 serine/threonine residues and at 5 tyrosine residues (7, 8, 11, 23). It is well established that the degree of phosphorylation of tau affects the ability of the protein to bind to microtubules and thereby stabilize the cytoskeleton (1).

The major serine/threonine kinases implicated in AD tau phosphorylation can be categorized as either proline- or non-proline-directed. The former includes glycogen synthase kinase (GSK)-3, cyclin-dependent kinase (CDK)-5 and the mitogen-activated protein kinase (MAPK) family. Non-proline-directed kinases include microtubule-affinity-regulating kinase (MARK), the casein kinase (CK)1 family and cyclic adenosine monophosphate (AMP)-dependent protein kinase (PKA). In addition, the non-receptor-linked tyrosine kinases, Fyn, c-abl and Syk, have been shown to phosphorylate tau [reviewed in (8)].

More recently, tau-tubulin kinase 1 (TTBK1) was identified as a brain-specific PKA that could phosphorylate tau at AD-related sites (16). TTBK1 is a dual serine/threonine and tyrosine kinase that is conserved among species. The nearest homologue to TTBK1 is TTBK2 (16) and both belong to the CK1 superfamily. TTBK1 has been shown, by partial phosphopeptide mapping, to phosphorylate tau at serine residues 198, 199, 202 and 422 and at tyrosine 197 *in vitro*, sites that are also phosphorylated in AD PHFs (7, 12). When co-expressed with tau in an intact cell system, only Ser199, Ser202 and Ser422 could be confirmed as TTBK1 substrates (16). TTBK2 has been shown to phosphorylate tau *in vitro* at Ser208 and Ser210, which are also found on AD PHFs (20).

TTBK1 is reported to be specifically expressed in the brain. Northern blotting of a human tissue panel showed TTBK1 mRNA in adult brain cortex and cerebellum, as well as in fetal brain. Weak expression of TTBK1 was detected in the spinal cord and testis. No apparent TTBK1 expression was seen in a range of other tissues, including heart, liver, kidney and lung. *In situ* hybridization (ISH) of mouse brain has shown TTBK1 gene expression in perinuclear and cytoplasmic regions of large cortical pyramidal cells in the temporal cortex cortical layers, CA1 layers of the hippocampus and granular layer of cerebellum. Immunohistochemistry (IHC) has confirmed neuronal expression of TTBK1 in both mouse and human brain (16).

In contrast to TTBK1, TTBK2 has been found in other tissues, including heart, muscle, liver, thymus, spleen, lung, kidney, testis and ovary (19, 20). In the mouse and rat brain, TTBK2 mRNA expression was found at high levels in the cerebellum and hippocampus as shown using ISH (10).

The function of TTBK1 with respect to AD pathogenic mechanisms has been studied by Sato *et al* who described transgenic TTBK1 mice in which the protein is highly expressed in subiculum and cortical pyramidal layers. TTBK1 mice show increased phosphorylation of both tau at Ser262/356 residues (12E8) and of neurofilament protein. The mice also showed significant age-dependent memory impairment as determined by a spatial learning radial arm water maze test. The fact that TTBK1 has not been shown to directly phosphorylate tau at Ser262/356 *in vitro* indicated that TTBK1 might enhance phosphorylation at this site either by activation of other kinases or through priming of tau by direct phosphorylation at other sites (17).

Subsequently, Xu *et al* used the same TTBK1 mice to generate bigenic mice that overexpress full-length TTBK1 and the disease-causing (FTDP-17) P301L tau mutant (24). These mice show accumulation of tau aggregates in cortical and hippocampal neurons at 12–13 months of age as well as enhanced tau phosphorylation as determined by AT8 (Ser202/205), 12E8 (Ser262/356), PHF-1 (Ser396/404) and Ser422. The phosphorylated tau aggregates were predominantly sarkosyl-soluble, consistent with small oligomers. The bigenic mice also showed significant locomotor dysfunction (a common phenotype of FTDP-17 mice), as well as enhanced loss of motor neurons.

The potential importance of TTBK1 in AD is supported by human genetic data from two independent association studies. Vázquez-Higuera *et al* analyzed nine TTBK1 gene single nucleotide polymorphisms (SNPs) in a group of Spanish AD patients and controls (22). Based on the data generated, it was speculated that reduced TTBK1 expression in minor allele homozygotes (rs2651206 in intron 1, rs10807287 in intron 5 and rs7764257 in intron 9) could lead to lower tau phosphorylation and NFT formation. Subsequently, Yu *et al* confirmed that minor alleles of the rs2651206 polymorphism were significantly associated with a reduced risk of late onset AD in a Han Chinese population (25).

To date, there is relatively little data on the mRNA and protein expression of TTBK1 in the human disease condition, although Sato *et al* did report levels of full-length and processed TTBK1 to be increased by c. 40% in frontal cortex homogenates of AD patients, as compared with age-matched controls (17). In the present study, we chose to characterize TTBK1 mRNA and protein expression in AD and control brains so as to provide more insight into the disease relevance of this novel kinase.

METHODS

Molecular biology

Plasmid cDNA for the overexpression of myc-tagged human TTBK1 was purchased from OriGene USA (Cat. No. RC214874; Acc. No: NM_032538.1; Rockville, MD, USA). For expression of human tau1-441, a synthetic DNA fragment was cloned downstream of a CMV promoter (GeneArt/Life Technologies, Carlsbad, CA, USA).

Cell culture and transfections

The human embryonic kidney cell line HEK293 was purchased from ATCC (CRL-1573, Manassas, VA, USA). Cells were grown in Dulbecco's modified Eagle's medium (DMEM)/F12 with Glutamax (Invitrogen, Carlsbad, CA, USA) supplemented with 10% heat-inactivated fetal calf serum (FCS; HyClone, Logan, UT, USA). Cells were seeded in 24-well culture dishes (Corning Inc., Corning, NY, USA) and transfected with a total of 0.8 μg plasmid cDNA/well at 80% confluence. Lipofectamine LTX with PLUS reagent (Invitrogen) was used for transfections according to the manufacturer's manual. Briefly, PLUS reagent was mixed with plasmid DNA in cell culture medium without serum and incubated for 5 minutes. Lipofectamine LTX was added and incubated for an additional hour. The complexes were added to the cells, and transfections were carried out for 24 h.

Sandwich immunoassay using Gyrolab workstation

Cells were lysed in buffer containing 50 mM Tris–HCl, pH 7.2, 150 mM NaCl, 1 mM ethylenediaminetetraacetic acid (EDTA), 1% Triton X-100, 10 mM NaF, 1 mM Na_3O_4V and 1 complete protease inhibitor cocktail tablet (Roche, Indianapolis, IN, USA)/10 mL buffer. The cells were incubated with lysis buffer for 5 minutes on ice before scraping from the wells. Samples were incubated at least overnight at −80°C before being thawed on ice and centrifuged at 14 000 rpm at 4°C. The supernatants were loaded onto a 96-well plate (Gyros AB, Uppsala, Sweden) and kept on ice until further use. The capture antibody against tau (tau-13, Abcam, Cambridge, UK) was biotinylated using the EZ link sulfo-NHS-LC biotinylation kit (Pierce, Rockford, IL, USA), while the detection antibodies against tau (HT7, Pierce), tau pSer422 (EPR 2866, Epitomics, Burlingame, CA, USA), tau pSer199 (1F3, AJ Roboscreen, Leipzig, Germany), tau pSer202/pThr205 (AT8, Innogenetics, Ghent, Belgium) and tau pSer231 (AT180, Innogenetics) were labeled using the Alexa Fluor 647 Antibody Labeling Kit (Invitrogen). The antibodies were loaded onto a 96-well plate (Gyros AB). The sample and antibody plates were loaded together with the Bioaffy 200 CD (Gyros AB) into the Gyrolab workstation with Degasser (Gyros AB), where after the instrument was started and operated according to manufacturer's instructions. In brief, samples and reagents were moved by the Gyrolab workstation to specific inlets on the CD, and then further moved through microstructures with streptavidin-coated beads by spinning the CD. Detection was performed using a laser-induced fluorescent detector integrated in the workstation.

Human tissue

All human tissue studies were reviewed and permitted by the appropriate ethical committee. Informed consent for donated tissue had been given by all patients or their next of kin.

All human brain tissue from AD patients and non-demented elderly controls were acquired from the Netherlands Brain Bank. Neuropathological diagnosis was based on NIA-Reagan criteria with a mixture of the Consortium to Establish a Registry for Alzheimer's Disease (CERAD) and Braak staging. Case and tissue details are summarized in Table 1. Brain tissue arrived as both

Table 1. Summary of cases included. Abbreviations: AD = Alzheimer's disease; CSF = cerebrospinal fluid; FF = fresh frozen; FFPE = formalin-fixed paraffin-embedded; HC = hippocampus; IFG = inferior frontal gyrus; NDE = non-demented elderly; PMI = post-mortem interval.

Case No.	Brain regions	Format	Gender	Age	Diagnosis	Braak stage	PMI (h:m)	pH CSF	Brain weight (g)	ApoE genotype
In situ hybridization										
1	HC, IFG	FF	M	74	NDE	0	8:00	6,75	1317	3:2
2	HC, IFG	FF	M	78	NDE	0	4:40	7,17	1259	3:3
3	IFG	FF	M	80	NDE	0	6:30	6,43	1285	3:3
22	IFG	FF	F	77	NDE	I	5:30	6.74	1343	4:3
4	HC, IFG	FF	M	78	NDE	I	6:55	6,42	1332	3:3
5	IFG	FF	F	81	NDE	I	6:40	7,16	1164	3:3
8	HC, IFG	FF	F	93	NDE	I	4:25	7,30	1223	3.2
23	IFG	FF	M	96	NDE	I	5:23	6,70	1204	3:3
11	HC, IFG	FF	F	71	AD	V	5:30	6,36	1125	4:3
24	HC, IFG	FF	M	75	AD	V	5:15	6,39	1178	4:3
12	HC, IFG	FF	F	84	AD	V	4:50	6,67	1092	4.4
16	HC, IFG	FF	F	88	AD	V	5:10	6,62	1075	4:3
20	HC, IFG	FF	M	87	AD	VI	3:25	7,75	1017	4:3
Immunohistochemistry										
7	IFG	FFPE	F	91	NDE	I	7:45	6,90	1074	3:3
25	HC	FFPE	M	87	NDE	II	4:55	6,31	1052	3:3
10	HC	FFPE	M	82	NDE	IV	10:00	6,53	1528	4:3
26	IFG	FFPE	F	86	AD	IV	5:05	6,62	998	4:3
14	HC	FFPE	F	84	AD	V	7:15	6,58	1129	4:3
27	IFG	FFPE	F	84	AD	V	5:55	6,42	1217	3:3
28	HC	FFPE	M	87	AD	V	6:10	6,14	1088	3:3
18	HC	FFPE	F	68	AD	VI	3:50	6,50	1095	3:2

formalin-fixed paraffin-embedded (FFPE) and fresh frozen (FF) blocks. FF tissue was sectioned on a cryostat in 8–10-μm slices, FFPE tissue on a microtome into 4-μm slices.

Synthesis of radioactive cRNA probes

^{35}S-UTP-labeled cRNA probes were synthesized by *in vitro* transcription with the MAXIscript Kit (Ambion, Austin, TX, USA) from a synthetic DNA fragment corresponding to parts of the coding exons 10–12 of human TTBK1 (560 bp, nucleotides 1105–1664 in the coding sequence of NM_032538) cloned into the pGEM-5Z (+) vector (GeneART). A pTRI-GAPDH Human Antisense Control Template was used as an mRNA quality control probe and purchased from Ambion. Transcription was driven by SP6 or T7 enzymes in both antisense and sense directions (only for TTBK1 probe) in the presence of TTP, GTP, CTP and ^{35}S-labeled UTP (MP Biomedicals, Illkirch, France).

The probe was designed so that it would be specific to TTBK1, with only 54% sequence identity towards TTBK2, the closest human homologue.

Following transcription, the DNA template was digested with DNAse. Riboprobes were subsequently purified using mini Quick Spin RNA columns (Roche). The quality of labeled riboprobes was verified qualitatively by TBE-urea gel electrophoresis and scintillation counting.

In situ hybridization

Both FF and FFPE tissues were tested for ISH, and FF tissue gave much higher signal to noise ratio and little problems with unspecific binding. Therefore, only FF tissue was used for this application. Slides were taken directly from the freezer and heated in an oven until completely dry. Slides were then fixed with 4% paraformaldehyde (PFA), rinsed three times with 2 × standard sodium citrate buffer (2 × SSC), equilibrated in 0.1 M triethanolamine and treated with 0.25% acetic anhydride in 0.1 M triethanolamine. After rinsing with 2 × SSC, slides were equilibrated in chloroform and dehydrated through an ethanol series (50–100%). Hybridization was performed in a buffer containing 60% formamide (Sigma, St. Louis, MO, USA), 365 mM NaCl, 12 mM Tris–HCl (pH 8,0), 1 mM EDTA, 1 × Denhardt's solution (Sigma), 12% dextran sulfate (Sigma), 0.5 mg/mL tRNA, 20 mM DTT and ^{35}S-labeled cRNA probe at 59°C overnight under a coverslip.

Following hybridization, slides were rinsed twice with 2 × SSC at room temperature, treated with 20 μg/mL RNase A for 30 minutes at 37°C, washed with a series of decreasing SSC-containing solutions with a final high stringency wash of 0.1 × SSC and 1 mM DTT at 69°C. Sections were then dehydrated and exposed to Kodak Biomax MR-2 film and dipped in NTB2 emulsion (Kodak, Rochester, NY, USA) and exposed at 4°C prior to development and counterstaining with hematoxylin.

Quantification of ISH

The ISH performed on sections from AD patients and non-demented controls was quantified by exposing slides to a Biomax MR autoradiography film (Kodak). The film was exposed for 7 days for TTBK1-probed tissue, 3 days for GAPDH. Film was developed and scanned, giving a low-resolution image of the mRNA expression of the brain sections. In every cassette, a slide

with a (^{14}C) autoradiographic microscale containing 31–883 nCi/g (Amersham LifeScience, Buckinghamshire, UK) was included. Autoradiography films were scanned in high resolution, and calculations of emission intensity done by the software Multigauge Ver 3.0 (FujiFilm, Tokyo, Japan). A standard curve was plotted based on the exposure of the film to the different amounts of known radiation in the microscales. Values were calculated as arbitrary units/square pixel. Gray matter of inferior frontal gyrus was the only area deemed homogenous enough to allow statistically relevant quantification. The amount of TTBK1 expression was estimated by dividing the average intensity of TTBK1 signal in a clearly defined anatomical area by the average intensity of GAPDH signal in exactly the same anatomical area on adjacent sections. Statistical significance was determined by Mann–Whitney *U*-test using GraphPad Software version 5 (GraphPad, La Jolla, CA, USA).

Brain tissues used for ISH were assessed for mRNA integrity with the GAPDH probe. The strength of mRNA signal was semi-quantitatively assessed by translating into a four-step scale, ranging from + to ++++, based on the low-resolution images. Only tissue that presented sufficient mRNA (having +++ or ++++ signal strength) was further used for ISH with probes to TTBK1 (a total of 22 of 57 tissue blocks). In doing so, mRNA integrity/tissue quality was ruled out as a factor when studying the mRNA level of genes with putative disease regulation, such as TTBK1.

Immunocytochemistry

HEK293 cells transiently expressing TTBK1 (previously described) were fixed in 4% PFA, pelleted, transferred into HistoGel (Richard-Allan Scientific, Kalamazoo, MI, USA) and paraffin-embedded. The FFPE block was sectioned at 4 μm on a microtome. For staining procedure, see IHC in the following statements.

Immunohistochemistry

Only FFPE sections were used for IHC because of better tissue morphology and decreased background staining compared with FF tissue. Immunohistochemical stainings were performed on either the Ventana Discovery XT automated staining module or the Dako Autostainer Link 48 with the OmniMap DAB kit (Ventana Medical Systems, Tucson, AZ, USA) or REAL EnVision Rabbit/Mouse kit (Dako, Glostrup, Denmark), respectively. FFPE sections were de-paraffinized and treated with an EDTA-based antigen retrieval solution (pH 7, 8 or 9). Endogenous peroxidase was blocked with 3% (FFPE) hydrogen peroxide. Tissue stained on the Dako Autostainer was taken through a protein-blocking step with a 0.25% casein/phosphate buffered saline (PBS) solution (DAKO Protein block). The following monoclonal antibodies were used: tau pSer202/pThr205 (AT8, Innogenetics), Aβ1-16 (6E10, Covance, Princeton, NJ, USA), Aβ17-24 (4G8, Covance), tau pSer422 (EPR2866, Epitomics), three-repeat (3R) tau (RD3, Millipore, Billerica, MA, USA), four-repeat (4R) tau (RD4, Millipore) and LAMP-1 (H4A3, Santa Cruz Biotechnology, Santa Cruz, CA, USA). The following polyclonal antibodies were used: TTBK1 C-term (SAB350002, Sigma), TTBK1 C-term2 (HPA031736, Atlas Antibodies, Stockholm, Sweden), TTBK1 N-term (AP4947a, Abgent, San Diego, CA, USA) and TTBK1 internal (sc-13331, Santa Cruz Biotechnology). All secondary antibodies were manufacturer-derived (Dako and Ventana) anti-mouse and anti-rabbit secondary antibodies conjugated to horseradish peroxidase (HRP). Visualization was done by addition of hydrogen peroxide and 3,3′-diaminobenzidine (DAB), giving an insoluble brown stain at the site of antibody binding. Finally, the tissue was counterstained with hematoxylin. To control for the specificity of the less well-characterized rabbit polyclonal antibodies, sections were stained in parallel with rabbit IgG, as well as without any primary antibody.

Double immunofluorescence

Double immunofluorescence was carried out manually according to the same protocol as previously mentioned but without peroxidase or protein blocking. Sections were stained with the first primary antibody and detected by incubation with Donkey anti-mouse FITC and Donkey anti-rabbit Cy3 conjugated secondary antibodies (Jackson ImmunoResearch, West Grove, PA, USA). The sections were stained in two steps, with separate incubations for the two primary antibodies.

Appropriate negative control stainings were performed in order to ascertain that the secondary antibodies only detected the appropriate primary antibody. Nuclei were stained with DAPI (Invitrogen).

Image acquisition for ISH and IHC

Slides were scanned with a NanoZoomer 2.0-HT slide scanner (Hamamatsu, Hamamatsu, Japan) in brightfield or fluorescence mode, and images were captured from the digital sections using NDP.view software.

RESULTS

Co-expression of TTBK1 and tau in HEK293 cells gives phosphorylation at the pSer422 and AT8 sites

When human tau and TTBK1 were co-expressed in the HEK293 cell line, strong phosphorylation of tau at the pSer422 (Figure 1A) and AT8 (Figure 1B) sites could be detected, as compared with cells transfected with tau alone. However, no change in the phosphorylation was detected at the pSer199 site (Figure 1C), which has also been implicated as a substrate for phosphorylation by tau. The relevance of these *in vitro* results was further strengthened by the fact that the Ser231 site, which is not considered a TTBK1 site of phosphorylation, was not affected by co-expression of tau with TTBK1 (Figure 1D). As control, total levels of tau were measured with a phosphorylation-insensitive antibody, demonstrating that TTBK1 co-transfection did not affect levels of total tau (Figure 1E).

TTBK1 mRNA is expressed in neuronal layers of AD patients and controls

To describe the cellular and anatomical expression of TTBK1, ISH was performed on sections of hippocampus and/or inferior frontal gyrus from five AD patients and eight non-demented controls (Table 1).

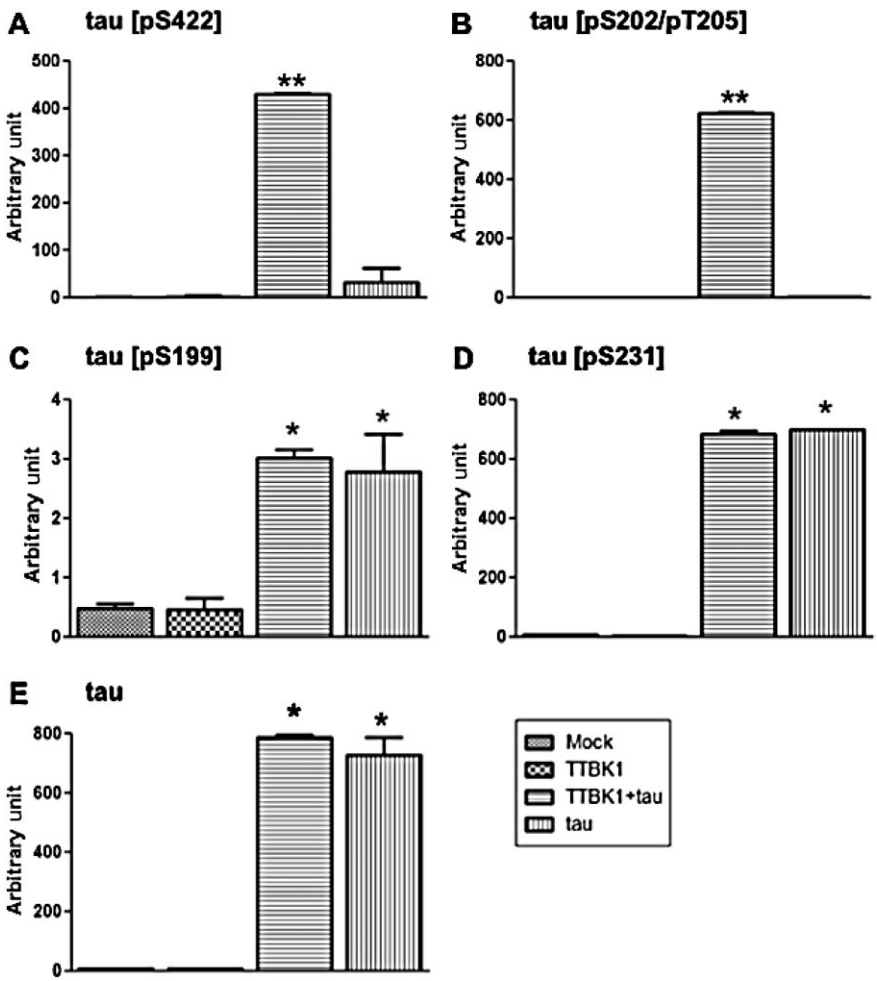

Figure 1. *Transfection of HEK293 with tau-tubulin kinase 1 (TTBK1) in combination with tau induces a specific increase in phosphorylation at pSer422 and AT8 sites on tau.* Transfection of mock, TTBK1, TTBK1 in combination with tau or tau cDNA plasmids was repeated twice, with two runs on Gyros in duplicate for both experiments. Values are means ± standard deviation, representative for both transfections. A specific increase of the pSer422 (**A**) and AT8 (**B**) epitopes is observed when TTBK1 is co-transfected with tau (TTBK1 + tau). No difference is observed in TTBK1 and tau co-transfection as compared with tau transfection alone (tau) at the pSer199 (**C**) and pSer231 (**D**) sites of tau. Levels of total tau (**E**) are unaffected by co-transfection with TTBK1 and levels of endogenous tau are low (mock and TTBK1). All epitopes were measured at the same time and collected from the same sample. All samples were diluted twice except for total tau measurements, where samples were diluted 20 times so as not to saturate the Gyros signal. *Significantly different against mock and TTBK1 transfections. **Significantly different against mock, TTBK1, and tau transfections; one-way ANOVA followed by Bonferroni post-hoc test, $P < 0.05$.

TTBK1 mRNA expression was high in both hippocampus and inferior frontal gyrus. In the hippocampus (Figure 2A), expression was abundant in entorhinal cortex and subiculum and particularly strong in the Cornu Ammonis (CA)-field and dentate gyrus (Figure 2B,C). Strong expression was detectable in several layers of frontal cortex (Figure 2D), with particularly strong expression being seen in larger pyramidal neurons. These expression patterns were observed in both AD cases and non-demented controls. TTBK1 mRNA expression was not detected in cell types other than neurons. When adjacent sections were stained with 6E10 + 4G8 and AT8 antibodies, it was evident that TTBK1 was expressed at high levels in neuronal populations where amyloid plaques and NFTs were abundant, such as the CA-fields and entorhinal (Figure 2A,B) and frontal (Figure 2D) cortices. Non-demented controls that completely lacked NFTs and plaques also displayed strong expression of TTBK1 in these neuronal fields. Quantification of expression in the cortical gray matter did not indicate any apparent difference in TTBK1 mRNA between AD cases and controls (Figure 2E). However, it should be noted that interindividual difference was quite pronounced. This was not caused by the overall mRNA quality in the tissue, as tissues had been pre-excluded if the mRNA level was low, as assessed on adjacent sections by the housekeeping gene *GAPDH*.

TTBK1 protein is restricted to the somatodendritic compartment of hippocampal and cortical neurons

In order to more specifically study the expression of TTBK1 on a cellular level, we screened a number of commercially available and in-house-produced antibodies toward human TTBK1. To verify the specificity of the antibodies, we stained HEK293 cells that had been transiently transfected with human TTBK1 cDNA (Figure 3A). Untransfected cells and rabbit IgG were used as negative controls. Antibodies were selected on their ability to selectively stain only the cells that had been transfected with human TTBK1. All antibodies were then used to stain sections of human frontal cortex. Again, a specific neuronal expression, similar to that observed with ISH, was evident with all antibodies tested (Figure 3B). The staining patterns were similar and ranged from diffuse to more granular staining in the somatodendritic compartment in all layers of the inferior frontal gyrus.

Particularly strong expression was observed with a C-terminal directed antibody (Sigma SAB350002). This antibody stained neurons in a dot-like granular manner in the somatodendritic compartment. Granular deposits were visible in the soma and preferentially found along the plasma membrane. Particularly strong

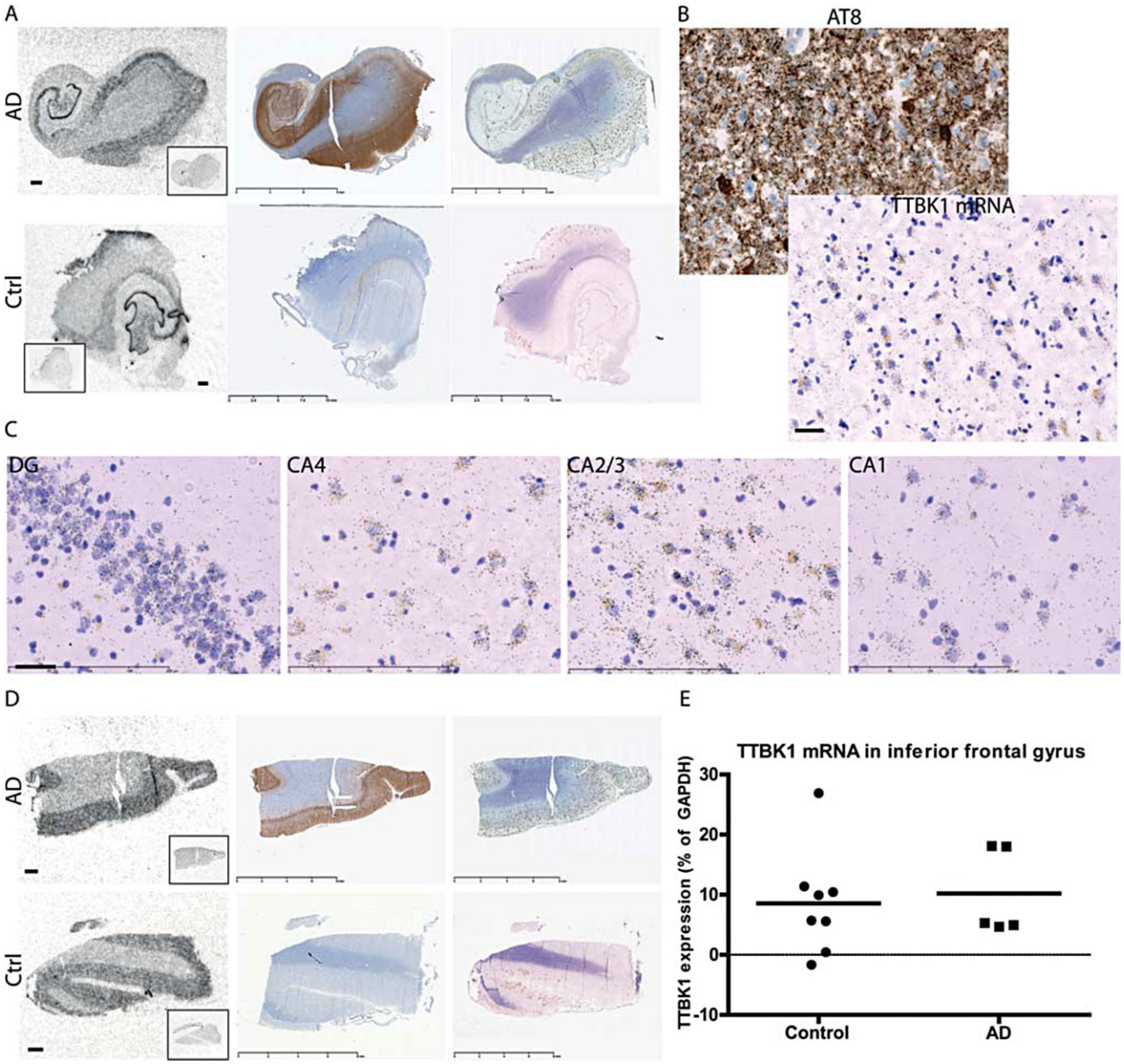

Figure 2. *Tau-tubulin kinase 1 (TTBK1) mRNA is evident in neuronal layers in both Alzheimer's disease (AD) and non-demented controls.* **A.** *In situ* hybridization against TTBK1 (left) revealed high expression in neuronal fields of the entire hippocampus of both AD cases (top) and non-demented elderly controls (bottom). In AD cases, TTBK1 expression was abundant in neuronal fields containing lots of phosphorylated tau (AT8, middle) and amyloid plaques (6E10/4G8, right). The same findings were made in non-demented controls that had very few NFTs and amyloid plaques. **B.** High-resolution image of adjacent sections demonstrating co-localization of TTBK1 mRNA and AT8 in the CA-field of an AD case (Braak V, case 20). **C.** High-resolution image demonstrating strong expression in all neuronal populations of the hippocampus (DG, CA4, CA2/CA3, CA1) as evidenced by silver grains accumulating in neuronal cells on emulsion dipped slides (non-demented Braak 0, case 4). **D.** In sections of inferior frontal gyrus, TTBK1 expression was high in all cortical layers, regardless of the level of phosphorylated tau and amyloid plaques. **E.** Quantification of mRNA expression in the gray matter of inferior frontal gyrus did not reveal any significant difference (as determined by Mann–Whitney *U*-test) between AD cases ($n = 5$) and non-demented controls ($n = 8$). Sections of hippocampus and inferior frontal gyrus in (A) and (D) are from one representative AD case (Braak VI, case 11) and one non-demented control (Braak 0, case 4). Inset images in the left panel are sections hybridized with the sense transcribed probe to control for labeling specificity. Scale bars: (**A**) 1 mm, (**B**) 200 μm, (**C**) 50 μm and (**D**) 1 mm.

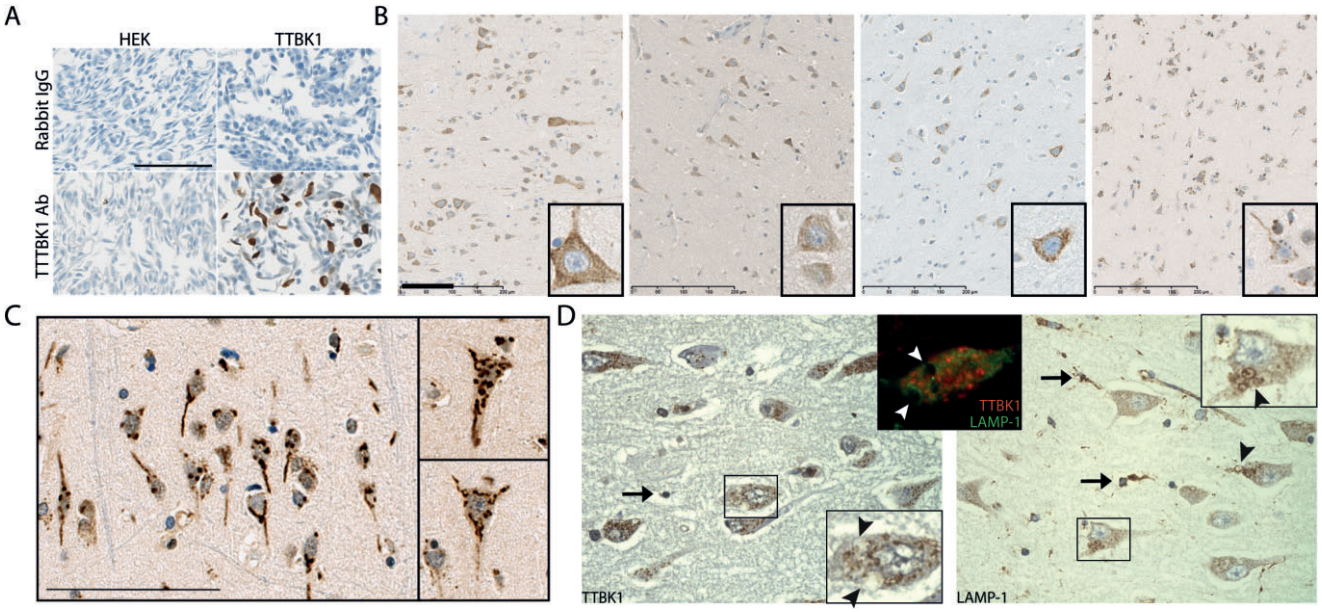

Figure 3. *Characterization of antibodies toward tau-tubulin kinase 1 (TTBK1).* **A.** HEK293 cells were transiently transfected with human TTBK1 cDNA (right) or untransfected (left) and subsequently stained with antibody to TTBK1 (bottom) or rabbit IgG as control (top) to assess the specificity of the antibody. Positive staining is only observed with the TTBK1 antibody on the TTBK1-transfected cells. **B.** Four antibodies toward TTBK1 (from left to right: HPA, Abgent, Santa Cruz and Sigma) had a similar staining pattern with immunoreactivity localized to the somatodendritic compartment of neurons in the frontal cortex. The Sigma antibody (**C)** produced particularly strong granular staining in the apical and basal dendrites and in deposits in the soma. **D.** Single and double staining of TTBK1 with a lysosomal marker (LAMP-1) in Alzheimer's disease (AD) hippocampus demonstrates that TTBK1 is not localized to lysosomes. LAMP-1 immunoreactivity is strong in glia (arrows) and diffuse in the cytoplasm of neurons. The membrane around granuvacuolar bodies (arrow heads) are strongly immunoreactive toward LAMP-1 but not to TTBK1. Double immunofluorescence confirms this lack of co-localization (inset). Scale bars: 100 μm.

immunoreactivity was visible at the apexes of the soma and in apical and basal dendrites. A "tail-like" staining in the apical dendrite was visible in practically all pyramidal neurons in the cortex (Figure 3C). Primary antibody control staining as well as rabbit IgG isotype control were completely negative in all brain tissue studied (data not shown).

As an early report suggested that TTBK1 is cleaved in the lysosome (16), we wanted to check whether the TTBK1-immunoreactive granules could be lysosomal structures. We stained hippocampal sections from an AD case with the TTBK1 antibody and a lysosomal marker (LAMP-1). We found that the LAMP-1 staining pattern was very dissimilar to that of the TTBK1 antibody. The LAMP-1 antibody stained glia very strongly (Figure 3D, arrows) and neurons more diffusely. Strong staining was observed in intraneuronal granuvacuolar bodies (Figure 3D, arrow heads), a structure where TTBK1 immunoreactivity was practically absent. This was confirmed by double immunofluorescence where almost no co-localization was observed (inset).

TTBK1 expression is abundant in pre-tangle neurons that are pSer422-immunoreactive

As we were able to confirm previous findings that TTBK1 can phosphorylate tau at the pSer422 site, and as this is a PHF-specific

Figure 4. *Tau-tubulin kinase 1 (TTBK1) co-localizes with pSer422-positive pre-tangles but not late-stage neurofibrillary tangles (NFTs).* Adjacent sections of hippocampus were stained with antibodies to pSer422 (left panel) and TTBK1 (right panel) in (**A**) an Alzheimer's disease (AD) case (Braak V, case 14), (**B**) a non-demented control (Braak II, case 25) and (**C**) a high-pathology non-demented control (Braak IV, case 10). TTBK1 immunoreactivity is strong in apparently healthy neurons without tau (arrow), as well as pre-tangle neurons with diffuse pSer422 staining and perinuclear immunoreactivity (arrowhead). Neurons containing dense aggregates of tau have almost no immunoreactivity to TTBK1 (red arrows). **D.** Single staining with antibodies toward 3R (RD3) and 4R (RD4) tau in an AD case (Braak V, case 28) reveal that these antibodies primarily stained late-stage NFTs (arrow heads, left column). Double-label immunofluorescence toward TTBK1 (Cy3, red) and AT8, RD3 or RD4 (FITC, green) showed again that TTBK1 immunoreactivity was practically absent from these mature NFTs (arrow heads), and that no association to tau isoform could be observed. However, TTBK1 did co-localize with AT8 in pre-tangle neurons (arrow), but was absent from neuropil threads. Scale bars: 50 μm.

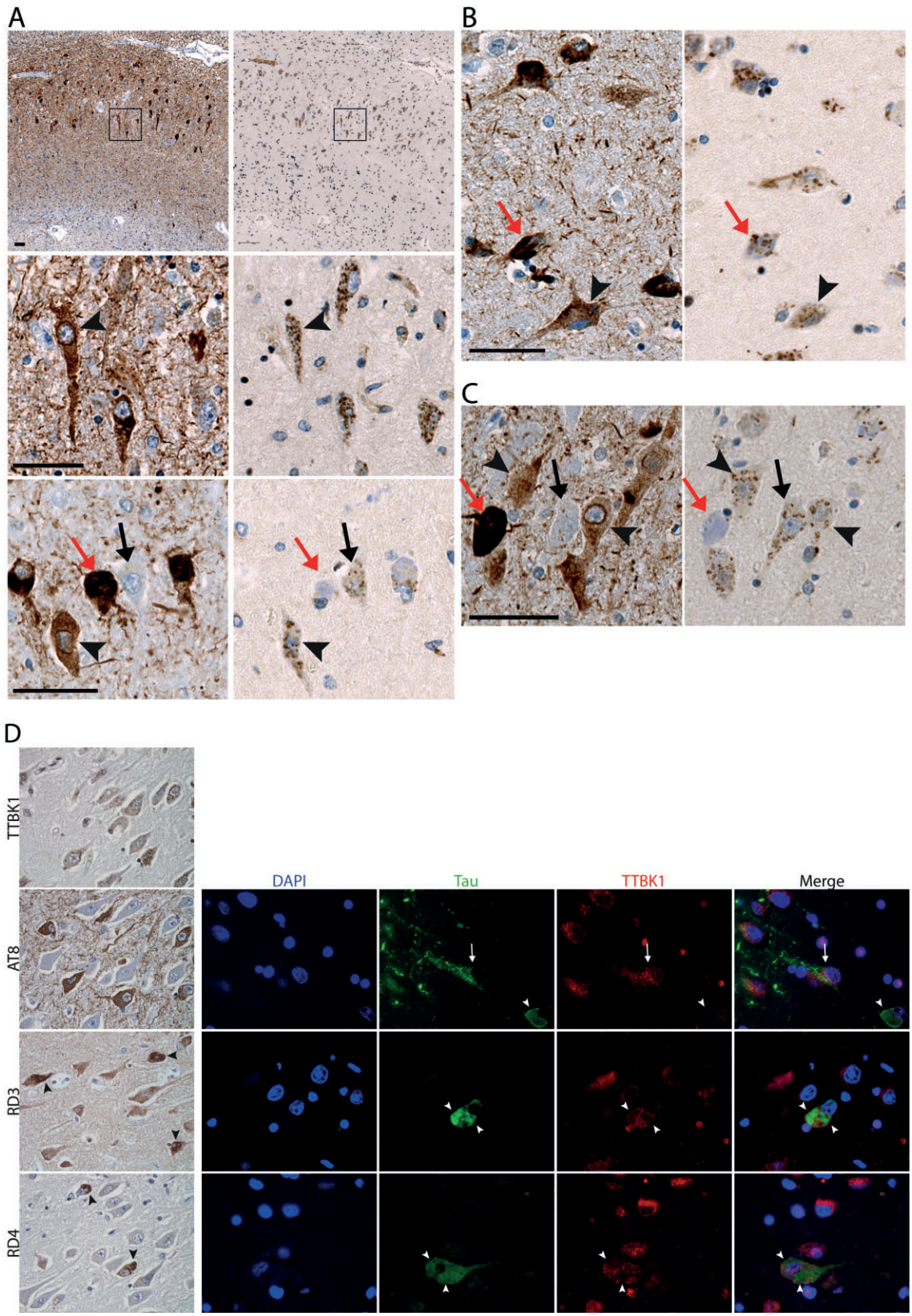

site that only few kinases can phosphorylate, we chose to compare the spatial co-localization of TTBK1 and pSer422 in the AD brain. To this end, we stained adjacent sections of hippocampus from several cases with different Braak stages (II, IV, V, VI) of tau pathology. The staining was performed on 4-μm-thin sections that were exactly adjacent, which allowed visualization of the same neuron in two separate sections.

TTBK1 immunoreactivity was only found in the soma and proximal parts of the apical and basal dendrites. In the CA-field, TTBK1 immunoreactivity was strong in healthy neurons without any accumulation of phosphorylated tau (Figure 4A–C, arrows), and intermediate in pre-tangle neurons. Pre-tangle neurons were characterized by diffuse pSer422 staining in the cytoplasm and a strong perinuclear staining (Figure 4A–C, arrowheads). Neurons containing dense accumulations of phosphorylated tau were less immunoreactive toward TTBK1 (Figure 4A–C, red arrows). The areas of the somatodendritic compartment that contained the most intense pSer422 labeling were as a rule completely devoid of any TTBK1 immunoreactivity. No co-localization was observed with pSer422-immunoreactive neuropil threads. As neuropil threads were too thin to visualize in adjacent sections, we confirmed these findings by double-label immunofluorescence of sections of frontal cortex with TTBK1 and AT8 antibodies. As we had already observed, TTBK1 co-localized with AT8 only in the somatodendritic compartment (data not shown) and did not co-localize with neuropil threads.

To address whether there was any association between TTBK1 and 3R or 4R tau isoforms, we performed double immunofluorescence of sections of hippocampus with TTBK1 and 3R- or 4R-specific antibodies RD3 and RD4, respectively. As control, we used AT8. Both RD3 and RD4 antibodies primarily stained neurons with dense tau aggregates (Figure 4D, arrow heads), and as we had previously observed, TTBK1 immunoreactivity was low or absent from these areas of the somatodendritic compartment (Figure 4D, arrow heads). No difference in the overlap with TTBK1 immunoreactivity could be observed between 3R or 4R isoforms. AT8 staining, on the other hand, co-localized with TTBK1 in pre-tangle neurons (Figure 4D, arrows). As we had seen before, no TTBK1 immunoreactivity was present in mature tangles (Figure 4D, arrow heads) or neuropil threads.

Characterization of pSer422 antibody identifies a rare population of AT8-unlabeled neurons

In order to characterize the pSer422 antibody toward the more well-established phospho-tau antibody AT8, double immunofluorescence was performed with the two antibodies on sections of hippocampus from one AD case (Braak VI) and one non-demented control (Braak II). The pSer422 antibody displayed an almost identical pattern to that of AT8, in that it stained NFTs (Figure 5A–D), neuropil threads and neuritic plaques (Figure 5E–H). However, rare exceptions were observed, where some neurons were only stained by the pSer422 antibody (Figure 5I–Q). These neurons were scattered throughout the hippocampal formation in the entorhinal cortex, and CA-field. In a hippocampus section from a Braak stage VI AD case, in which several hundred NFTs are found, as few as 22 neurons were found that were single-labeled with the pSer422 antibody.

DISCUSSION

A large number of kinases have been identified as having the ability to phosphorylate tau both *in vitro* and *in vivo* (18). However, the individual contribution to tau phosphorylation by these kinases in the AD brain is largely unknown. GSK3 and CDK5 are suspected to play a major role in pathological phosphorylation of tau in the brain. As such, large efforts have been made to develop inhibitors toward these kinases (4). One of the main disadvantages of targeting such kinases is their ubiquitous expression in the rest of the body, which could give serious unwanted peripheral side effects. TTBK1 therefore appears to be a potentially attractive candidate for pharmacological inhibition because of its apparent restricted expression to neurons in the CNS. Furthermore, TTBK1 has a dual phosphorylation ability, being both a serine/threonine and a tyrosine kinase. TTBK1 was able to phosphorylate eight sites of tau *in vitro*, among them Tyr197. Phosphorylation of tyrosines has been demonstrated in PHF-tau (23), and this has been suggested to be an early event in PHF formation (12). TTBK1 is the only kinase that has been able to phosphorylate Tyr197. However, Tyr197 phosphorylation could not be confirmed when tau was co-expressed with TTBK1 in an intact cell system (16), although the authors suggest that detection could have been hampered by interference from phosphorylated serine residues 198 and 199. Only Ser199, Ser202 and Ser422 could be confirmed when tau was co-expressed with TTBK1 in COS-7 cells.

We chose only to study these confirmed phosphorylation sites in our cell system. When we carried out a similar experiment in the human cell line HEK293, we detected robust phosphorylation at the Ser422 and AT8 (Ser202/Thr205) sites. However, the Ser199 site, which has been shown to be phosphorylated by TTBK1 *in vitro* (16), did not result in any changes in our assay system. Ser231, which is not known to be phosphorylated by TTBK1, was used as a negative control, and no change in phosphorylation could be detected at this site when tau was transfected either alone or in combination with TTBK1.

Having confirmed the ability of TTBK1 to phosphorylate tau *in vitro*, we then mapped the mRNA and protein expression of this kinase in post-mortem brain from AD and control cases. Using ISH, we were able to detect abundant mRNA in neuronal cells of both AD cases and non-demented controls. No apparent mRNA expression was seen in other non-neuronal cell types. TTBK1 mRNA appeared to be present in those neuronal fields with high levels of plaques and tangles. However, signals were equally strong in control cases without signs of pathological changes. We could not detect any apparent statistically significant difference in TTBK1 mRNA levels in frontal inferior gyrus of AD cases and controls.

Having confirmed the localization of TTBK1 mRNA to neurons in the human brain, we then studied protein expression. A previous study has demonstrated increased levels of TTBK1 protein in AD cortical brain homogenates compared with controls (17), although the intracellular localization of TTBK1 has not been studied previously in detail. To this end, we screened a panel of antibodies toward TTBK1. Four antibodies identified by their ability to label HEK293 cells transfected with hTTBK1, all stained neurons in sections of human inferior frontal gyrus with diffuse or granular immunoreactivity in the somatodendritic compartment. The difference in staining pattern could be explained by the different

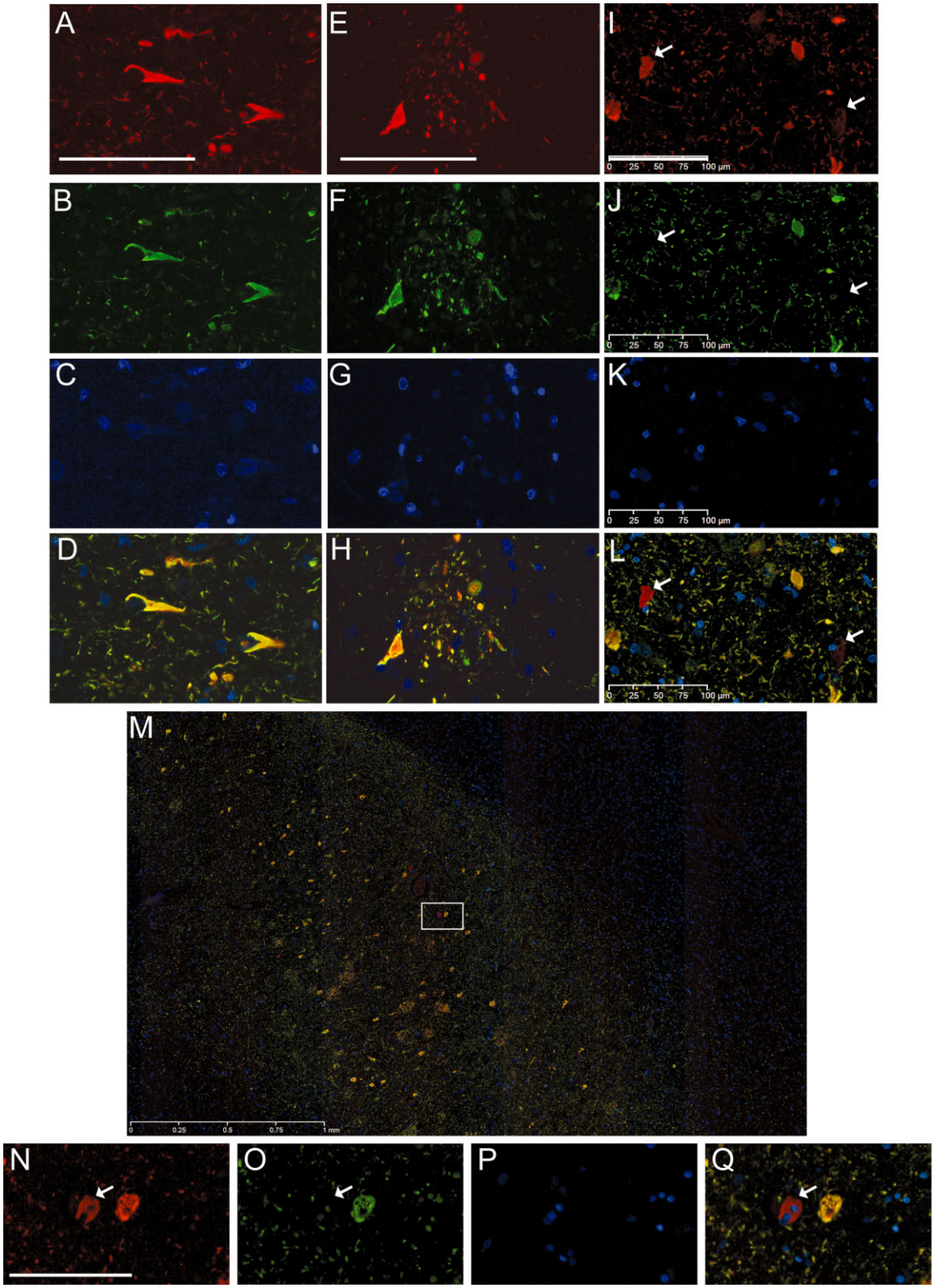

Figure 5. *A unique population of neurons is single-labeled with a phospho-specific antibody toward pSer422.* Double immunofluorescence in the CA-field of hippocampus from an (**A**–**L**) Alzheimer's disease (AD) case (Braak VI, case 18) and a (**M**–**Q**) non-demented control (Braak II, case 25) with pSer422 (Cy3, red) and AT8 (FITC, green) demonstrates that both antibodies labeled neurofibrillary tangles (NFTs) (**A**–**D**), and neuritic plaques and neuropil threads (**E**–**H**) but revealed a small population of neurons that are single-labeled with the pSer422 antibody (**I**–**L** and **M**–**Q**, arrows). Scale bars: 100 µm.

epitopes that the antibodies are directed toward, as well as the use of different epitope retrieval treatments. A C-terminal-directed antibody (SAB350002) produced the strongest immunoreactivity in cortical and hippocampal neurons and was therefore used for co-staining with pSer422. Strong granular immunoreactivity associated with the plasma membrane, nucleus and apical dendrite was observed. Although TTBK1 is suggested to be processed in the lysosome (16), we did not observe any co-localization with a lysosomal marker. We interpret the staining pattern to suggest that TTBK1 is associated with the microtubule network in the soma and proximal parts of apical/basal dendrites. Indeed, Sato *et al* demonstrated co-localization of TTBK1 with β3-tubulin (16). Phosphorylation of tau by TTBK1, if it occurs *in vivo*, is therefore most likely to occur in the somatodendritic compartment. Indeed, strong staining was observed in pre-tangle neurons with diffuse pSer422 immunoreactivity in the soma. Additionally, we did not observe any colocalization of TTBK1 with neuropil threads. As tau has been suggested to be miss-sorted from axons to the somatodendritic compartment as it aggregates (3, 13), and we could not detect any TTBK1 in mature NFTs, this indicates a role for TTBK1 in pre-tangle formation, when tau is starting to sequester in the cell body. The absence of TTBK1 in late-stage NFT neurons could also reflect lack of space, epitope masking within the aggregate or neuronal death. An alternative explanation is that TTBK1 protects against the formation of mature NFTs.

When we characterized the pSer422 antibody in relation to AT8, we found a very high degree of overlap. When double immunofluorescence was carried out, a small population of neurons were identified that were single-labeled with the pSer422 antibody. In contrast, no neurons were single-labeled with the AT8 antibody.

This is in line with a previous report (2) claiming that Ser422 becomes phosphorylated earlier in the development of an NFT, preferentially marking intracellular NFTs. Here, we show that, although this may be the case in a few examples, the vast majority of NFTs are immunolabeled with both antibodies. We interpret this to mean that NFT formation is a rapid process, and that the progression from pre-tangle to mature NFT occurs quickly. This is also in line with a recent *in vivo* two-photon imaging study in a transgenic mouse model of tauopathy, showing that tangle formation occurred in a matter of days (5). TTBK1 is one of few kinases, along with the MAPKs, that can phosphorylate tau at Ser422 (14–16). It has been shown to be a very specific marker for pathological PHF-tau, with only little phosphorylation being present in the normal adult brain (9).

Interestingly, a recent active immunization study toward the Ser422 site demonstrated reduced levels of insoluble tau paralleled by improved cognition in a Y-maze test in a mouse model of tauopathy (21). These studies along with the present one suggest that interfering with tau phosphorylation at Ser422 would be a good therapeutic strategy in arresting tau phosphorylation before tangle formation is possible.

Interestingly, both TTBK1 and TTBK2 can phosphorylate tau at sites that are found in PHFs (16, 20). One would therefore expect that an upregulation or overactivation of each one of these kinases would lead to increased tau phosphorylation and predispose to neurodegeneration. Indeed, genetic variations in TTBK1, which are thought to result in decreased TTBK1 activity, can decrease the risk of AD (22, 25). However, loss of function mutations in TTBK2 causes spinocerebellar ataxia with severe neurodegeneration of cerebellar Purkinje neurons (10). This could reflect alternate roles for TTBKs in development and aging. Alternatively, TTBK1 and TTBK2 may have opposing functions in neurodegeneration, where TTBK1 promotes disease and TTBK2 protects.

In summary, we here confirm that TTBK1 can phosphorylate tau at Ser422, and that it is indeed a neuron-specific kinase in the human brain, primarily expressed in the somatodendritic compartment where it co-localizes with pSer422 pre-tangle neurons but not late-stage NFTs.

ACKNOWLEDGMENTS

All human brain tissue used in this study was obtained from the Netherlands Brain Bank, Amsterdam (Dr Inge Huitinga).

REFERENCES

1. Alonso AC, Zaidi T, Grundke-Iqbal I, Iqbal K (1994) Role of abnormally phosphorylated tau in the breakdown of microtubules in Alzheimer disease. *Proc Natl Acad Sci U S A* **91**:5562–5566.
2. Augustinack JC, Schneider A, Mandelkow EM, Hyman BT (2002) Specific tau phosphorylation sites correlate with severity of neuronal cytopathology in Alzheimer's disease. *Acta Neuropathol (Berl)* **103**:26–35.
3. Binder LI, Frankfurter A, Rebhun LI (1985) The distribution of tau in the mammalian central nervous system. *J Cell Biol* **101**:1371–1378.
4. Brunden KR, Ballatore C, Crowe A, Smith AB, 3rd, Lee VM, Trojanowski JQ (2010) Tau-directed drug discovery for Alzheimer's disease and related tauopathies: a focus on tau assembly inhibitors. *Exp Neurol* **223**:304–310.
5. de Calignon A, Fox LM, Pitstick R, Carlson GA, Bacskai BJ, Spires-Jones TL, Hyman BT (2010) Caspase activation precedes and leads to tangles. *Nature* **464**:1201–1204.
6. Grundke-Iqbal I, Iqbal K, Tung YC, Quinlan M, Wisniewski HM, Binder LI (1986) Abnormal phosphorylation of the microtubule-associated protein tau (tau) in Alzheimer cytoskeletal pathology. *Proc Natl Acad Sci U S A* **83**:4913–4917.
7. Hanger DP, Betts JC, Loviny TL, Blackstock WP, Anderton BH (1998) New phosphorylation sites identified in hyperphosphorylated tau (paired helical filament-tau) from Alzheimer's disease brain using nanoelectrospray mass spectrometry. *J Neurochem* **71**:2465–2476.
8. Hanger DP, Seereeram A, Noble W (2009) Mediators of tau phosphorylation in the pathogenesis of Alzheimer's disease. *Expert Rev Neurother* **9**:1647–1666.
9. Hasegawa M, Jakes R, Crowther RA, Lee VM, Ihara Y, Goedert M (1996) Characterization of mAb AP422, a novel phosphorylation-dependent monoclonal antibody against tau protein. *FEBS Lett* **384**:25–30.
10. Houlden H, Johnson J, Gardner-Thorpe C, Lashley T, Hernandez D, Worth P *et al* (2007) Mutations in TTBK2, encoding a kinase implicated in tau phosphorylation, segregate with spinocerebellar ataxia type 11. *Nat Genet* **39**:1434–1436.
11. Iqbal K, Liu F, Gong CX, Alonso Adel C, Grundke-Iqbal I (2009) Mechanisms of tau-induced neurodegeneration. *Acta Neuropathol (Berl)* **118**:53–69.
12. Lebouvier T, Scales TM, Williamson R, Noble W, Duyckaerts C, Hanger DP *et al* (2009) The microtubule-associated protein tau is also phosphorylated on tyrosine. *J Alzheimers Dis* **18**:1–9.
13. Li X, Kumar Y, Zempel H, Mandelkow EM, Biernat J, Mandelkow E (2011) Novel diffusion barrier for axonal retention of tau in neurons and its failure in neurodegeneration. *EMBO J* **30**:4825–4837.

14. Reynolds CH, Nebreda AR, Gibb GM, Utton MA, Anderton BH (1997) Reactivating kinase/p38 phosphorylates tau protein in vitro. *J Neurochem* **69**:191–198.
15. Reynolds CH, Utton MA, Gibb GM, Yates A, Anderton BH (1997) Stress-activated protein kinase/c-jun N-terminal kinase phosphorylates tau protein. *J Neurochem* **68**:1736–1744.
16. Sato S, Cerny RL, Buescher JL, Ikezu T (2006) Tau-tubulin kinase 1 (TTBK1), a neuron-specific tau kinase candidate, is involved in tau phosphorylation and aggregation. *J Neurochem* **98**:1573–1584.
17. Sato S, Xu J, Okuyama S, Martinez LB, Walsh SM, Jacobsen MT *et al* (2008) Spatial learning impairment, enhanced CDK5/p35 activity, and downregulation of NMDA receptor expression in transgenic mice expressing tau-tubulin kinase 1. *J Neurosci* **28**:14511–14521.
18. Sergeant N, Bretteville A, Hamdane M, Caillet-Boudin ML, Grognet P, Bombois S *et al* (2008) Biochemistry of tau in Alzheimer's disease and related neurological disorders. *Expert Rev Proteomics* **5**:207–224.
19. Takahashi M, Tomizawa K, Sato K, Ohtake A, Omori A (1995) A novel tau-tubulin kinase from bovine brain. *FEBS Lett* **372**:59–64.
20. Tomizawa K, Omori A, Ohtake A, Sato K, Takahashi M (2001) Tau-tubulin kinase phosphorylates tau at Ser-208 and Ser-210, sites found in paired helical filament-tau. *FEBS Lett* **492**:221–227.
21. Troquier L, Caillierez R, Burnouf S, Fernandez-Gomez FJ, Grosjean ME, Zommer N *et al* (2012) Targeting Phospho-Ser422 by active tau immunotherapy in the THYTau22 mouse model: a suitable therapeutic approach. *Curr Alzheimer Res* **9**:397–405.
22. Vázquez-Higuera JL, Martinez-Garcia A, Sanchez-Juan P, Rodriguez-Rodriguez E, Mateo I, Pozueta A *et al* (2011) Genetic variations in tau-tubulin kinase-1 are linked to Alzheimer's disease in a Spanish case-control cohort. *Neurobiol Aging* **32**:550 e5–550 e9.
23. Vega IE, Cui L, Propst JA, Hutton ML, Lee G, Yen SH (2005) Increase in tau tyrosine phosphorylation correlates with the formation of tau aggregates. *Brain Res Mol Brain Res* **138**:135–144.
24. Xu J, Sato S, Okuyama S, Swan RJ, Jacobsen MT, Strunk E, Ikezu T (2010) Tau-tubulin kinase 1 enhances prefibrillar tau aggregation and motor neuron degeneration in P301L FTDP-17 tau-mutant mice. *FASEB J* **24**:2904–2915.
25. Yu NN, Yu JT, Xiao JT, Zhang HW, Lu RC, Jiang H *et al* (2011) Tau-tubulin kinase-1 gene variants are associated with Alzheimer's disease in Han Chinese. *Neurosci Lett* **491**:83–86.